Journal of Magnetism and Magnetic Materials 456 (2018) 241–250

Contents lists available at ScienceDirect

Journal of Magnetism and Magnetic Materials

journal homepage: www.elsevier.com/locate/jmmm

Research articles

Propagation of magnetostatic spin waves in an yttrium iron garnet film for out-of-plane magnetic fields

Wonbae Bang [a], Jinho Lim [a,*], Jonathan Trossman [a], C.C. Tsai [b], John B. Ketterson [a,c]

[a] *Department of Physics and Astronomy, Northwestern University, Evanston, IL 60208, USA*
[b] *Department of Engineering & Management of Advanced Technology, Chang Jung Christian University, Tainan 71101, Taiwan*
[c] *Department of Electrical and Computer Engineering, Northwestern University, Evanston, IL 60208, USA*

A R T I C L E   I N F O

Article history:
Received 1 October 2017
Received in revised form 9 February 2018
Accepted 10 February 2018
Available online 14 February 2018

Keywords:
Spin wave propagation
YIG
Out-of-plane
Exchange branches

A B S T R A C T

We have observed the propagation of spin waves across a thin yttrium iron garnet film on (1 1 1) gadolinium gallium garnet for magnetic fields inclined with respect to the film plane. Two principle planes were studied: that for **H** in the plane defined by the wave vector **k** and the plane normal, **n**, with limiting forms corresponding to the Backward Volume and Forward Volume modes, and that for **H** in the plane perpendicular to **k**, with limiting forms corresponding to the Damon-Eshbach and Forward Volume modes. By exciting the wave at one edge of the film and observing the field dependence of the phase of the received signal at the opposing edge we determined the frequency vs. wavevector relation, $\omega = \omega(\mathbf{k})$, of various propagating modes in the film. Avoided crossings are observed in the Damon-Eshbach and Forward Volume regimes when the propagating mode intersects the higher, exchange split, volume modes, leading to an extinction of the propagating mode; analysis of the resulting behavior allows a determination of the exchange parameter. The experimental results are compared with theoretical simulations.

1. Introduction

One can distinguish three different "classes" of spin waves in thin ferromagnetic films, depending on the orientation of the magnetic field (**H**), the film normal (**n**), and the wavevector (**k**), where the latter lies in the sample plane. For the first two of these the amplitude extends throughout the thickness of the film and hence they are referred to as volume modes. The geometry in which **H** is parallel to **k** supports a so called Backward Volume mode (BV mode) which has the unusual property that the group velocity (v_g) and **k** are oppositely directed (and hence its name). The geometry in which **H** is parallel to **n** supports a Forward Volume mode (FV mode); here v_g and **k** are aligned. The third mode involves a geometry in with **H**, **n**, and **k** are mutually perpendicular: this wave is called the Damon-Eshbach mode (DE mode) after the investigators who first clarified its nature, and it is concentrated at one of the two *opposing* film surface and decays exponentially into the bulk; reversing the field changes the sign of **k** and concentrates the wave on the other surface. One of these surfaces can be free while the other is adjacent to the substrate on which the film was grown.

In this paper, we report theoretical simulations and experimental results on the angular dependence of spin wave transmission at angles lying between the FV and BV geometry, and between the FV and DE geometry in the long wavelength limit. Furthermore, we report a study of interactions between magnetostatic branches and exchange branches [1–10]. The case involving the coupling of a FV branch and an exchange branch was treated by Wolfram and De Wames [9] who considered both a metallic magnetic layer and an insulating magnetic layer. The case involving the DE mode and an exchange branch was treated by Andreev et al. [3]; they investigated how this interaction depends on the film thickness as well as the relative orientation of wave vector with respect to a crystallographic orientation. Adam et al. [2] showed the interaction for the first case is stronger than the second, however they did not provide a quantitative comparison between those interactions. Here we calculate a coupling strength from our model allowing us to report a ratio of the coupling strength for the two cases.

2. Experimental method

All experiments were performed on either of two nominally identical yttrium iron garnet (YIG) films grown epitaxially on a (1 1 1) gadolinium gallium garnet (GGG) substrate which were supplied by the MTI Corporation. The film had dimensions of 5 mm by 10 mm and a stated thickness of 3.05 μm. Experiments

* Corresponding author.
E-mail address: JinhoLim15.2014@u.northwestern.edu (J. Lim).

https://doi.org/10.1016/j.jmmm.2018.02.030
0304-8853/

were carried out for spin wave propagation along both the long (10 mm) and short (5 mm) dimensions of the film.

The spin waves were generated and detected by 50 μm diameter wires running adjacent to opposing but nominally parallel edges of the film. The field generated by passing a microwave current through the transmitting wire couples to a spin wave of the corresponding frequency via two mechanisms: electromagnetic boundary conditions at the film edge and the gradient of the field generated by the wire. The first is judged to be the dominant mechanism and there is no natural short-wavelength cut-off associated with it. However, the "straightness" of the launched wavefront is limited by edge roughness. Similar mechanisms act at the opposing (receiving) edge of the film; however, here phase cancellation can occur across the arriving wavefront, if this edge is not parallel to the transmitting edge from which the wave is launched, an effect that becomes more pronounced at shorter wavelengths.

Fig. 1(a) and (b) show, schematically, two different experimental setups that were utilized in this work. Fig. 1(a) shows the "single ended" setup, which was used to determine the magnetic field, field-angle, and microwave-frequency dependence of the FMR position. Here, we used a sample holder with a single 50 μm diameter Cu wire running along one edge of the film; single ended measurements were also carried out with the wire passing over the interior of the film to distinguish any edge effects. One end of the wire was connected to a Hewlett Packard HP 8360 Series Synthesized Sweeper, operating in the range 10 MHz–20 GHz and at power levels up to 25 dBm, while the opposing end of the wire was connected to a microwave diode detector. All measurement functions (sweeping the field together while recording the magnetic field and lock-in output) were carried out via a personal computer operating under LabView. The d.c. magnetic field was supplied by a 6 in. Varian electromagnet driven by a pair of Kepco 20 A bipolar operational amplifier power supplies operating in the constant current mode; the field was swept at fixed microwave frequencies. Measurements could also be carried out by sweeping the frequency at fixed field; this mode has the accompanying effect of folding the frequency response of the transmitting and receiving antennas together with that of all interconnecting components (e.g. the interconnecting coaxial cables) into the overall response, which must then be corrected for. The magnet fields were measured with a Bell 5180 Hall probe with a digital output which was read by the computer. Additionally, the magnetic field was modulated at 380 Hz resulting in an a.c. output of the diode that was, in turn, detected with a Princeton 124 lock-in amplifier, the overall signal then being proportional to the derivative of the microwave absorption as the magnetic field is swept. An example of such data is shown Fig. 4(a) and Fig. 7(a). The experiments were repeated for various angles in a range of 3–9 GHz.

Fig. 1(b) shows, schematically, the two-wire "transmission" setup that was used for the measurements of spin wave

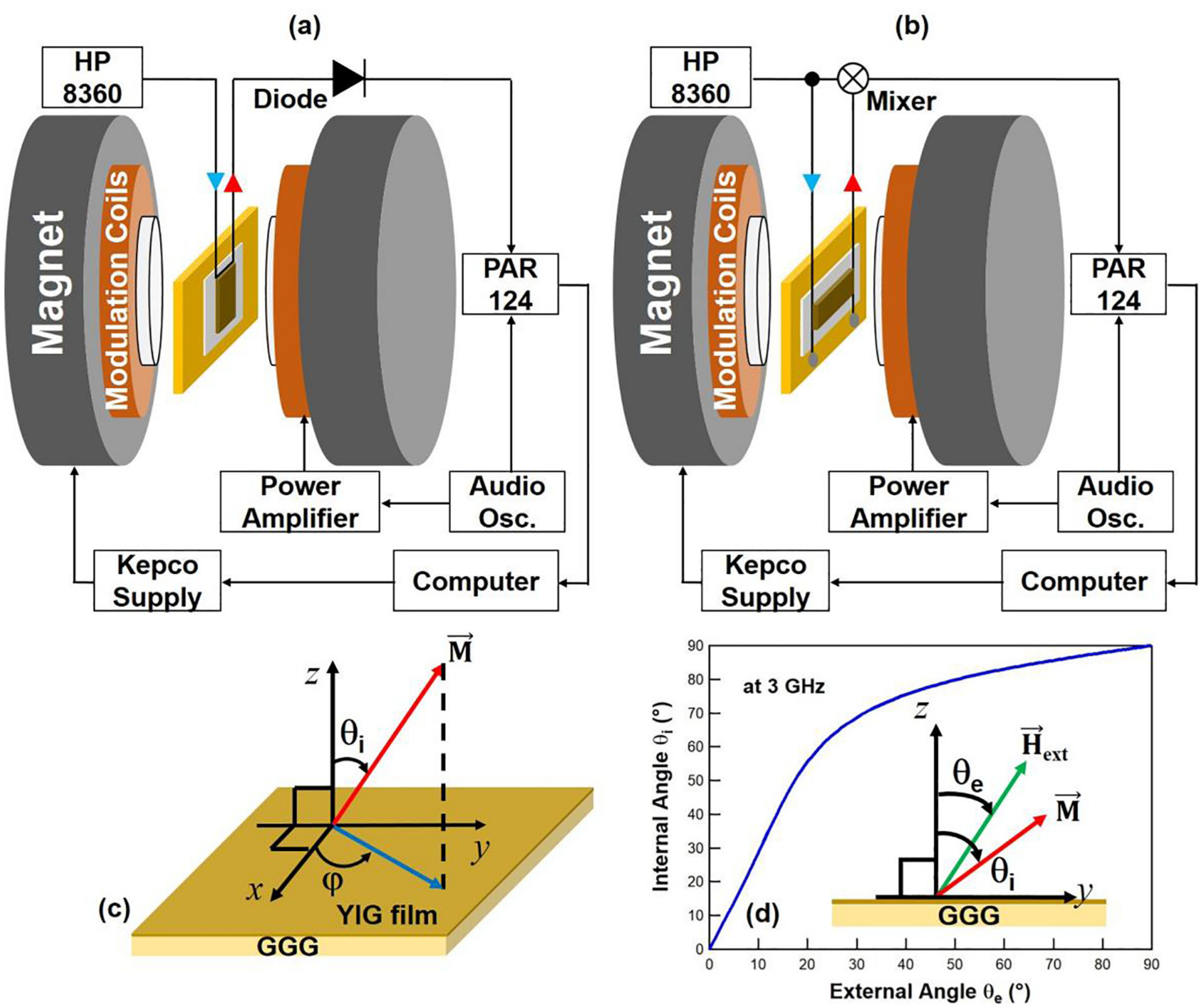

Fig. 1. (a) A schematic of the experimental setup for the FMR position measurement and (b) for phase detection measurement which is representative of a FV geometry in FV-BV setup. The geometry of the system is shown in (c) and (d). We choose sample normal as the *z*-axis and the direction of **k** as *y*-axis.